

# Principle of a dual-band search coil magnetometer: a new instrument to investigate magnetic fields fluctuation in space.

C. Coillot, J. Moutoussamy, G. Chanteur  
CETP/CNRS  
10-12, Avenue de l'Europe – 78140 Vélizy –France  
[christophe.coillot@cetp.ipsl.fr](mailto:christophe.coillot@cetp.ipsl.fr)

**Abstract—** Search-coil magnetometers are still often used in space physics thanks to their ability to measure weak magnetic field (few tens of  $fT/\sqrt{Hz}$  at kHz) and also their robustness. However, their frequency band is limited by the resonance of the coil. A second coil, used to extend the frequency band, is almost inefficient after the resonance of the first coil. We present a solution, called “mutual reducer”, to make it able to extend frequency band. The physical principle is described. The “dual-band” magnetic sensor so-designed will be on board, for the first time, on Bepicolombo mission which aims to investigate Mercury’s magnetosphere.

## I. INTRODUCTION

Usually, two kinds of magnetometers [1] are required on scientific spacecraft mission to fulfill scientific objectives: fluxgates are well adapted for weak magnetic field from DC to a few Hz, while search coils<sup>2</sup> extend the frequency band measurement from few 100 mHz to few kHz. These instruments are dedicated to contribute to the characterization of space plasma in order to provide a better understanding of such vast problems as dynamics of the terrestrial magnetosphere in the solar wind [2], [3]. Fluxgates are well known to be very sensitive for low frequency magnetic field measurement (typically until 10Hz). Then, design of search coil is related to the requirement of achieving a Noise Equivalent Magnetic Induction (NEMI) at 10Hz which extend fluxgate measurement (typically  $10pT/\sqrt{Hz}$  at 1Hz).

In the context of exploratory space missions, where environment and behaviour are misunderstood, a wide range of physical data is required (physical quantities, dynamic range and frequency range) in spite of restrictions such as mass budget and power consumption of the instruments. For Bepicolombo mission, physical phenomenon such as Alfvén waves, whistler waves and solar burst are expected with magnetic signature in a wide frequency range from few mHz up to 1MHz. This objective has led us to investigate

the search-coil magnetometer with extended frequency band ability.

## II. SEARCH COIL BASIS

Search coil principle is based on a magnetic core, which amplifies external magnetic field ([4], [5]), combined to a coil wound around an optimized core shape [6] (figure 1). This coil amplifies the induced voltage due to the flux variation inside the magnetic core. Then, the sensor is associated with a very low noise preamplifier [7], [8]. In addition a feedback loop is used to crush the sensor natural resonance [7], which leads to a transfer function as represented on figure 2.

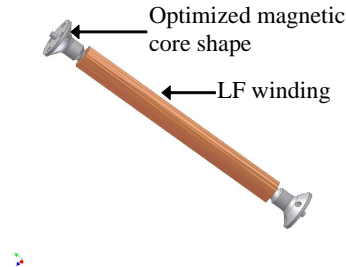


Figure 1. search coil sensor with optimized magnetic core shape.

Let us first consider a sensor designed to reach  $2pT/\sqrt{Hz}$  at 10Hz, its characteristics are: optimized core shape (with relative permeability:  $\mu_{ri}=2500$ ), 100mm length, 4mm diameter and 14000 turns. The NEMI of this low frequency (LF) search coil decreases while frequency increases until resonance occurs (around 2kHz for the curve on figure 2 with crushed resonance due to the use of a feedback loop). Above the resonance frequency NEMI increases, so the NEMI of such a sensor will not allow measurement of weak magnetic field up to few 10 kHz which is necessary to investigate unknown magnetosphere such as Mercury one.

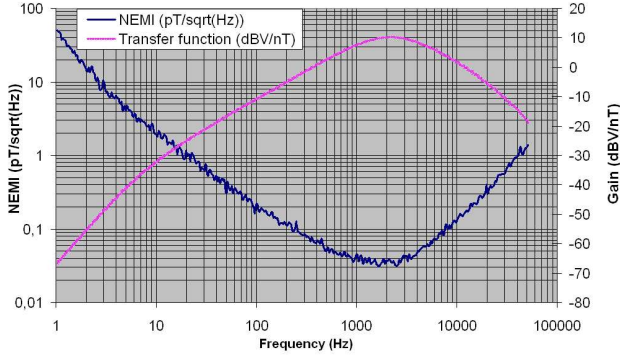


Figure 2. Transfer function and NEMI curve of a LF search coil.

### III. FREQUENCY BEHAVIOR DISCUSSION

Induced voltage which appears on the winding is:

$$e(t) = -N_1 \frac{d\phi(t)}{dt} \Rightarrow E = N_1 S \langle \mu_{app} \rangle \omega B, \quad (1)$$

where  $e = E e^{j\omega t}$ ,  $N_1$  is the turn number,  $S$  is the core section,  $\omega = 2\pi f$  is the pulsation,  $\langle \mu_{app} \rangle$  is the average apparent permeability and  $B$  is the flux density. Next induced voltage is compared to noise sources (thermal noise  $4kTR_1$  and voltage noise from amplifier  $e_{PA}$ ):

$$(N_1 S \langle \mu_{app} \rangle \omega B)^2 = e_{PA}^2 + 4kTR_1 \quad (2)$$

NEMI is then defined as the smallest magnetic field ( $B$ ) which can be detected beyond the noise:

$$NEMI = \frac{\sqrt{e_{PA}^2 + 4kTR_1}}{N_1 S \mu_{app} \omega} \quad (3)$$

From (3) it can be deduced that NEMI of search coil is improved (i.e. NEMI is smaller) when frequency increases. In order to reach a NEMI value at a given frequency (in our case  $2\text{pT}/\sqrt{\text{Hz}}$  at  $10\text{Hz}$ ), one can use (3) to compute required turn number ( $N$ ). Then, we assume that sensor behaves like RLC circuit (Figure 3.). More modeling details are given in [6], [7] and [8]. From equivalent circuit of figure 3 one can deduce transfer function between output voltage and external magnetic field:

$$T(j\omega) = \frac{V}{B} = \frac{-j\omega N_1 S \mu_{app}}{(1 - L_1 C_1 \omega^2) + jR_1 C_1 \omega} \quad (4)$$

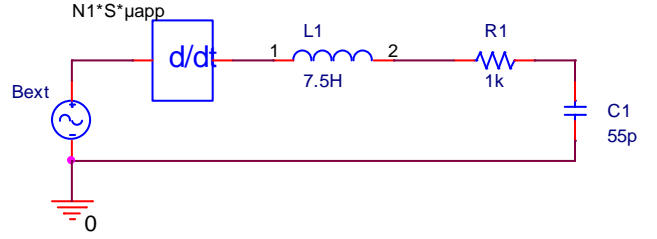


Figure 3. Equivalent electrical circuit of search coil.

Transmittance of search coil permits to express more accurately NEMI frequency behavior:

$$NEMI = \frac{\sqrt{e_{PA}^2 + 4kTR_1}}{N_1 S \mu_{app} \omega} \sqrt{(1 - L_1 C_1 \omega^2)^2 + (R_1 C_1 \omega)^2} \quad (5)$$

Equation (5) of NEMI shows clearly that above resonance frequency (i.e.  $\omega < \sqrt{1/LC}$ ) the induced voltage is reduced from the capacitive behavior of the sensor while NEMI value increases (i.e. becomes worst).

### IV. FEASIBILITY OF SEARCH COIL USING TWO WINDINGS ON A SAME MAGNETIC CORE TO EXTEND FREQUENCY RANGE

Obviously, first idea is to use a second winding with a higher resonance frequency to extend the frequency range measurement. Let us examine an “intuitive” design of such a winding (referred as “HF” winding). The design of such winding is obtained by translating the NEMI curve on the figure 2 to the starting point of the desired extended frequency band. We consider a LF band which stops at  $10\text{kHz}$ . From figure 2 we deduce a NEMI equal to  $100\text{fT}/\sqrt{\text{Hz}}$  which gives us the starting point of the design of the HF winding. Then, from (3) we can extrapolate the design of the HF coil. We consider the magnetic core is the same and equivalent noise is also the same. So on, we express the turn number of the HF coil from the turn number of the LF coil, multiplied by the ratio of two frequencies (6). These frequencies correspond to the frequency  $\omega_1$  such as NEMI for the LF is  $100\text{fT}/\sqrt{\text{Hz}}$ , that is approximately  $200\text{Hz}$  (from figure 2) and the frequency  $\omega_2$  such as NEMI for the HF is  $100\text{fT}/\sqrt{\text{Hz}}$ , that is  $10\text{kHz}$  (as desired).

$$N_2 \approx N_1 \frac{\omega_1}{\omega_2} \approx \frac{N_1}{50} \quad (6)$$

Such winding has been implemented in two configurations. First, the HF winding,  $N_2=280$  turns, has been implemented on a magnetic core alone. Second, the HF winding has been implemented on the complete search coil sensor (LF winding on magnetic core) and what happens?

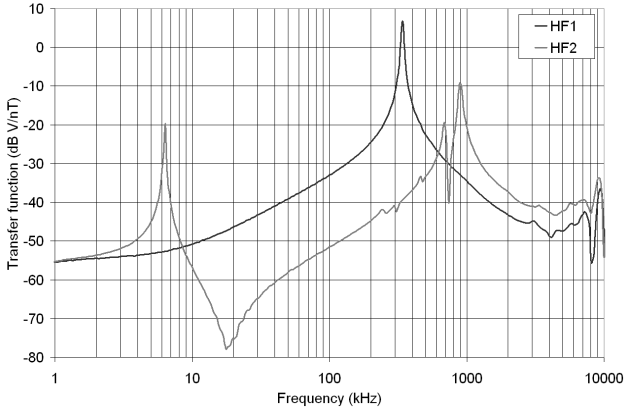


Figure 4. Transfer functions for HF winding on a magnetic core (HF1) and HF winding on a magnetic core associated to LF winding (HF2).

When the HF winding is realized directly on a magnetic core, his behavior is compliant with expected one (4). Transfer function (HF1 curve on Figure 4) increases until the resonance occurs at 300 kHz, then transfer function decreases due to the capacitive behavior of the winding. On the other hand, when a LF winding is wound on the magnetic core (HF2 curve on Figure 4), the HF winding exhibits an induced voltage which increases until the resonance frequency of the LF winding occurs (at about 6 kHz). Above this frequency an anti-resonance occurs and induced voltage increases but remains 20dB below what is obtained for the HF winding alone on the magnetic core. To understand this phenomenon, let us express magnetic flux of each winding. Index 1 and 2 represent respectively LF and HF winding.

$$\phi_1 = N_1 B \mu_{app} S + L_1 I_1 + M_{21} I_2 \quad (7)$$

$$\phi_2 = N_2 B \mu_{app} S + L_2 I_2 + M_{12} I_1 \quad (8)$$

The current flowing the LF winding ( $I_1$ ), is given by:

$$I_1 = -\frac{N_1 B S \mu_{app} j \omega}{R_1 + j L_1 \omega + 1/(j C_1 \omega)} \quad (9)$$

For frequency lower than resonance frequency the current value is weak. After resonance frequency, the main contribution in the impedance value of the winding comes from the inductive part:  $j L_1 \omega$ . Equation (9) becomes:

$$I_1 \approx -\frac{N_1 B S \mu_{app}}{L_1} \quad (\text{when } \omega > 1/\sqrt{L_1 C_1}) \quad (10)$$

Simplified expression of the current (10) is substituted inside (8), which becomes:

$$\phi_2 = N_2 B \mu_{app} S + L_2 I_2 - M_{12} \frac{N_1 B \mu_{app} S}{L_1} \quad (11)$$

$$\phi_2 = (N_2 - \sigma N_2) B \mu_{app} S + L_2 I_2 \quad (12)$$

Coefficient  $\sigma$  represents a mutual coupling coefficient between the two windings. When, windings are realized on a same magnetic core, this coefficient  $\sigma$  is almost 1 and we obtain:

$$\phi_2 \approx L_2 I_2 \quad (13)$$

In this latter expression, part of the flux which is dependant of magnetic field has disappeared and the magnetic field can not be measured with a second winding after the resonance of the first one. In such a way a second winding on a same magnetic core is inefficient to extend frequency band measurement.

## V. PHYSICAL DESCRIPTION OF A MUTUAL REDUCER

In order to extend frequency range measurement with an HF winding it will be needed to reduce mutual coupling from one winding on the other one. The original way we propose to do that, consists in using a magnetic material which surrounds the first winding as described on figure 5. This "mutual reducer" permits to the self-induction flux of the LF winding to find a path through the mutual reducer (red lines on figure 6). It results, that self-induction flux from LF winding seen by HF winding is considerably decreased.

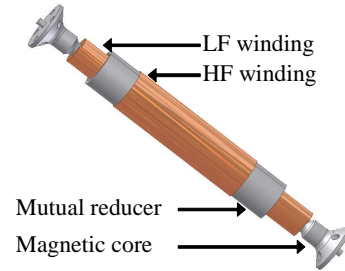


Figure 5. dual-band search coil magnetometer consists in two winding on a magnetic core separated by a cylindrical magnetic core (mutual reducer).

Another consequence is that apparent permeability are now different for the two windings ( $\mu_{app}$  is replaced either by  $\mu_{app1}$  for LF winding or by  $\mu_{app2}$  for HF winding). Values of the apparent permeability ( $\mu_{app1}$  and  $\mu_{app2}$ ) mainly depend on the shape of the mutual reducer. The parameters of the sensor: mutual induction coefficient, auto-induction and apparent permeability can be obtained from

numerical computation with electromagnetism software. Then, the expression of flux under HF winding becomes:

$$\phi_2 = N_2 \mu_{app2} B_{ext} S_2 - L_2 I_2 - M_{12} \frac{N_1 \mu_{app1} B_{ext} S_1}{L_1} \quad (11)$$

$$\phi_2 = \mu_{app-eq} N_2 B_{ext} S_2 - L_2 I_2 \quad (11)$$

$$\mu_{app-eq} = \mu_{app2} - \frac{M_{12} N_1}{L_1 N_2} \mu_{app1} \frac{S_1}{S_2} \quad (11)$$

This equation shows that mutual coupling must be lower as possible to makes the apparent permeability ( $\mu_{app-eq}$ ) higher as possible. The auto induction flux will not compensate the flux created by the magnetic field to be measured. As shown on figure 6 the magnetic field lines from auto-induction close through the mutual reducer. That implicates that flux from auto-induction is not completely seen under HF winding. Since a part of this flux is derived through the mutual reducer, this part is subtracted. So on, the resulting flux from auto-induction of LF coil is reduced thanks to the mutual reducer.

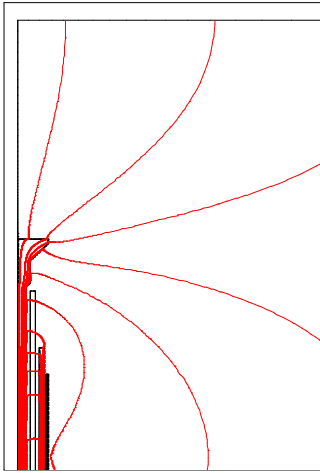


Figure 6. Self-induction magnetic field lines with a mutual reducer

The transfer function measurement for an HF winding combined to a mutual reducer is presented on figure 7 (curve HF3). The HF3 curve is close to the expected curve (HF1). However a mutual coupling with LF winding remains. The signature of this residual coupling is seen through the resonance which occurs at about 5 kHz. The HF behavior so obtained makes possible measurement of weak magnetic field from 10kHz until 1M Hz with the HF winding.

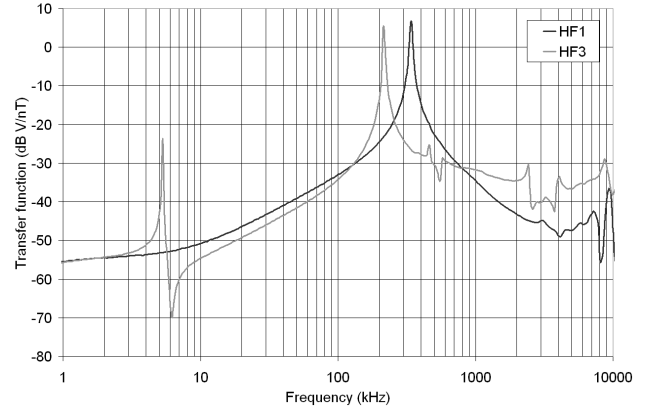


Figure 7. mesures d'un bobinage HF sur noyau magnétique (HF1) et d'un bobinage HF sur noyau magnétique avec bobinage BF et découpleur de flux (HF3)

## VI. CONCLUSION

The dual-band search-coil magnetometer on board on Bepicolombo will be able to measure magnetic field from Hz up to 640kHz thanks to the original use of a mutual reducer described in this paper. Sensor is 10cm long, 2cm diameter and weight 60grams. The low NEMI of this sensor on a wide frequency range ( $100\text{fT}/\sqrt{\text{Hz}}$ ) from 200 Hz to 640kHz will allow to measure expected and unexpected magnetic signature in the Mercury's magnetosphere.

## ACKNOWLEDGMENT

The authors would like to thank CNES who financially support the realization of this sensor and Pr Matsumoto for having welcomed this magnetometer in the plasma wave consortium of Bepicolombo mission.

## REFERENCES

- [1] P. Ripka, "Magnetic sensors and magnetometers", Artech house-Norwood (2001), pp. 57-65.
- [2] F.F. Chen, "Introduction to plasma physics", 2<sup>nd</sup> Edition, Plenum press, 1984.
- [3] N. Cornilleau-Wehrin et al., "First results obtained by the Cluster STAFF experiment", *Annales Geophysicae*, **21**, 2, 437-437.
- [4] J.A. Osborn, "Demagnetizing factors of the general ellipsoids", *Physical Review* (June 1945), Vol 67, p. 351.
- [5] R.M. Bozorth – D.M. Chapin, "Demagnetizing factor of rods", *Journal of applied physics*, n°13, may 1942, 320-327 (TBC)
- [6] C. Coillot, J. Moutoussamy, P. Leroy, G. Chanteur, A. Roux, "Improvements on the design of search coil magnetometer for space experiments", *sensor letters*, Vol 5, N° 1, march 2007, pp 167-170.
- [7] H.C. Seran, P. Fergeau, "An optimized low frequency three axis search coil for space research", *Review of Scientific Instruments*, **76**, 044502 (2005).
- [8] D.G. Lukoschus, "Optimization theory for induction-coil magnetometers at higher frequencies", *IEEE Transactions on geoscience electronics* (July 1979), Vol GE-17, n°3, pp56-63.